Anderson model with spin-flip-associated tunneling

Kao-Chin Lin and Der-San Chuu
Department of Electrophysics, National Chiao-Tung University, Hsinchu 300, Taiwan
(Received 3 March 2005; revised manuscript received 11 July 2005; published 9 September 2005)

The spin-flip-associated transport through a quantum dot based on the Anderson model in equilibrium and nonequilibrium situations is studied. It is found that electrons are scattered due to the spin-flip effect via the normal and the Kondo channels. Our results show that the conductance is suppressed due to the spin-flip effect, and the suppression due to the spin-flip scattering via the Kondo channel is stronger for temperatures below the Kondo temperature.

DOI: 10.1103/PhysRevB.72.125314 PACS number(s): 73.23.−b, 73.63.−b, 75.25.+z

I. INTRODUCTION

Recently, much theoretical and experimental research related to electron spin has been done. Owing to the progress in nanofabrication and microelectronic techniques, devices based on the electron spin, such as spin memory,[1] spin transistor,[2] and electron-spin-based quantum computers,[3,4] may be realized very soon. These devices are related to the spin-polarization orientation or spin-flip effect. Usually, the spin-flip effect occurs in scattering processes. The scattering processes may be caused by magnetic impurities, magnons, or domain walls at the interface or electrode,[5] or may be due to interactions with phonons[6] or the photon field.[7] In addition to scattering processes, spin flip may occur when the electron is transported between different spin-state regions. One of the instances is that the electron is transported between the Rashba quantum dot and the ferromagnetic lead. The Rashba effect can be observed in InAs semiconductors. The eigenstate of the Rashba Hamiltonian is a superposition of the spin states $|\uparrow\rangle$ and $|\downarrow\rangle$, i.e., $|\pm\rangle=(1/\sqrt{2})(e^{i\theta/2}|\uparrow\rangle\pm e^{-i\theta/2}|\downarrow\rangle)$.[4] It is known that the off-diagonal terms of the tunneling amplitude matrix and coupling constant are nonzero and spin-flip-associated tunneling appears in the system.[8] A sketch of the spin-flip-associated tunneling through a quantum system is shown in Fig. 1.

The spin-flip-associated tunneling effect might cause some special behaviors in the electric properties of the material. The intradot spin-flip effect was found to shift the resonant energy ϵ_0 of the quantum dot to $\epsilon_0\pm R$, where R is the spin-flip scattering amplitude.[8] Sergueev *et al.*[9] studied the spin-flip-associated tunneling through a quantum dot and described the spin-valve effect. The spin-valve effect caused by the transport between different spin states shows that the resistance depends on the direction (parallel or antiparallel) of the magnetization of two ferromagnetic metals.[9–12] Zhu and Balatsky studied the spin-flip-associated tunneling through a local nuclear spin precessing in a magnetic field to simulate the conductance oscillation observed in STM experiments.[13] They included the off-diagonal process and concluded that the conductance of the system can be obviously modified. Guinea pointed out that elastic spin-flip effects give rise to a temperature-independent reduction of the magnetoresistance while inelastic spin-flip processes give rise to temperature-dependent non-Ohmic effects and variation of the conductance.[5] As mentioned above, the spin-flip effect is important in the study of spin electronic devices and thus is worth exploring.

In spin-based devices such as a spin-based quantum computer, which may be operated at low temperature, the correlation between the electron in the quantum dot and the conduction electrons in the reservoir is important because the correlation will cause a peak of the density of states in the vicinity of the Fermi level for temperature $T\leqslant T_K$, where T_K is the Kondo temperature. The Anderson impurity model, which describes the correlation due to on-site Coulomb interaction and the direct tunneling between the conduction band and the local spin state in the magnetic impurity, is also employed to describe the quantum dot (QD) system.[14] The correlation interaction causes a sharp peak in the vicinity of the Fermi level for temperatures below T_K. The electron in the impurity may tunnel out of the impurity site to occupy a "virtual state," and then be replaced by an electron from the metal.[15,16] This process can effectively "flip" the spin of the impurity. Schrieffer and Wolff have shown that, in the limit of strong on-site Coulomb interaction, the Anderson impurity model is equivalent to the *s-d* model when the impurity level ϵ_0 is well below the Fermi level and the Kondo effect is obtained in this limit.[17] In the original Anderson impurity model, the electron spin does not flip during the process of tunneling between the impurity and the electron reservoir. In this work, we consider that the electron spin flips during the tunneling process, i.e., the spin-flip-associated coupling constant $\Gamma_\alpha^{\bar{\sigma}\sigma}=2\pi\Sigma_{k,s,\alpha\in L,R}V^*_{k_\alpha s,\bar{\sigma}2}V_{k_\alpha s,\sigma}\delta(\omega-\epsilon_{k\alpha s})$ where $\sigma(s)$ is the spin state of the electron in the QD (lead) and $\bar{\sigma}\neq\sigma$ is included in our study. The effects on the density of states and the conductance of the quantum dot system versus the strength of the spin-flip coupling will be discussed. Compared to the original Anderson model, the spin-flip-associated tunneling effect is expected to contribute additional self-energy which may modify the local density of state (LDOS), or the diagonal part of the spectral function $-2\,\mathrm{Im}\,G^r_{\sigma\sigma}$. The conductance depends strongly on the profile of the diagonal part of the spectral function $-2\,\mathrm{Im}\,G^r_{\sigma\sigma}$ and the off-diagonal part of the spectral function $-2\,\mathrm{Im}\,G^r_{\bar{\sigma}\sigma}$, which may change sign in the vicinity of the peak position of the LDOS. Therefore, the off-diagonal spectral function is expected to modify the conductance. In other words, the conductance may be modified by spin-flip-associated tunneling.

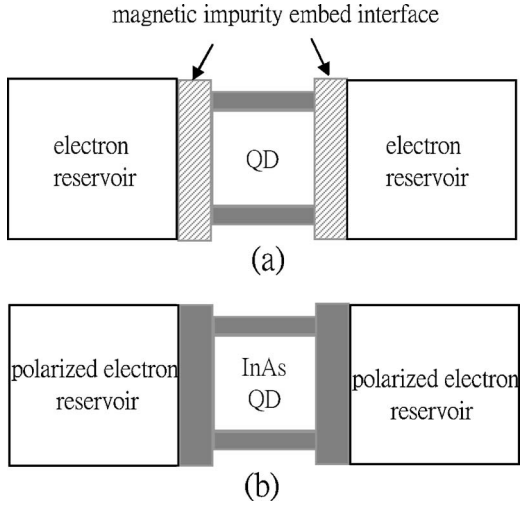

FIG. 1. The schematic plot of the system considered in this work. The spin-flip-associated tunneling is (a) originated by the impurity scattering and (b) due to the tunneling between the different spin states.

Instead of studying the mechanism of the spin-flip effect, we will study the spin-flip effect in a phenomenological way. The tunneling coupling constant will be assumed the same as that proposed in Ref. 13.

II. MODEL AND FORMALISM

The Hamiltonian of the system considered in this work can be written as

$$H_d = \sum_{\sigma} \epsilon_{\sigma} d_{\sigma}^{\dagger} d_{\sigma} + U n_{\sigma} n_{\bar{\sigma}},$$

$$H_C = \sum_{\substack{k_{\alpha} s \\ \alpha \in L,R}} \epsilon_{k_{\alpha} s} c_{k_{\alpha} s}^{\dagger} c_{k_{\alpha} s},$$

$$H_T = \sum_{k_{\alpha} s,\sigma} V_{k_{\alpha} S,\sigma}^{*} d_{\sigma}^{\dagger} c_{k_{\alpha} s} + V_{k_{\alpha} S,\sigma} c_{k_{\alpha} s}^{\dagger} d_{\sigma} \tag{1}$$

where $d_{\sigma}^{\dagger}(d_{\sigma})$ is the creation (annihilation) operator of the electron with spin state σ in the dot, and $c_{k_{\alpha} s}^{\dagger}(c_{k_{\alpha} s})$ is the creation (annihilation) operator of an electron with momentum k and spin state s in the α lead (where $\alpha \in L,R$). Note that the spin states s and σ are not necessary in the same eigenstate, for example, the spin state σ in the QD may be the eigenstate of the Rashba state and the spin state s in the lead may be the pure spin-up or spin-down state. The energy $\epsilon_{k_{\alpha} s}$ is the single-particle energy of the conduction electron in the α lead. U is the intradot Coulomb interaction. The electron tunneling between the lead and dot can be described by the tunneling matrix $V_{k_{\alpha} s,\sigma}$. As shown in Ref. 13, the coupling constant between the QD and the lead can be expressed by $\Gamma_{\alpha}^{\bar{\sigma}\sigma} = 2\pi \Sigma_{k,s,\alpha \in L,R} V_{k_{\alpha} s,\bar{\sigma}}^{*} V_{k_{\alpha} s,\sigma} \delta(\omega - \epsilon_{k\alpha s})$. The spin-flip coupling constant is set to be symmetric for the state $\sigma(\bar{\sigma})$ flipped into the state $\bar{\sigma}(\sigma)$, i.e., $\Gamma_{\alpha}^{\bar{\sigma}\sigma} = \Gamma_{\alpha}^{\sigma\bar{\sigma}} = \Gamma_{\alpha}^{s}$. And the normal coupling constant $\Gamma_{\alpha}^{\sigma\sigma} = 2\pi \Sigma_{k,s,\alpha \in L,R} V_{k_{\alpha} s,\sigma}^{*} V_{k_{\alpha} s,\sigma} \delta(\omega - \epsilon_{k\alpha s})$ is assumed to be spin independent, i.e., $\Gamma_{\alpha}^{\sigma\sigma} = \Gamma_{\alpha}^{\bar{\sigma}\bar{\sigma}} = \Gamma_{\alpha}^{n}$. In this paper, we use the notation $\bar{\sigma}$ to stand for the spin being not equal to σ while σ' is equal or not equal to σ.

The Green's function **G** corresponding to the spin-flip-associated tunneling effect of the noninteracting system can be written as

$$\begin{bmatrix} G_{\sigma\sigma} & G_{\sigma\bar{\sigma}} \\ G_{\bar{\sigma}\sigma} & G_{\bar{\sigma}\bar{\sigma}} \end{bmatrix} = \begin{bmatrix} G_{\sigma\sigma}^{0} & 0 \\ 0 & G_{\bar{\sigma}\bar{\sigma}}^{0} \end{bmatrix} + \begin{bmatrix} G_{\sigma\sigma}^{0} & 0 \\ 0 & G_{\bar{\sigma}\bar{\sigma}}^{0} \end{bmatrix} \begin{bmatrix} \Sigma_{\sigma\sigma} & \Sigma_{\sigma\bar{\sigma}} \\ \Sigma_{\bar{\sigma}\sigma} & \Sigma_{\bar{\sigma}\bar{\sigma}} \end{bmatrix} \begin{bmatrix} G_{\sigma\sigma} & G_{\sigma\bar{\sigma}} \\ G_{\bar{\sigma}\sigma} & G_{\bar{\sigma}\bar{\sigma}} \end{bmatrix}$$
$$= \begin{bmatrix} [(G_{\sigma\sigma}^{0})^{-1} - \Sigma_{\sigma\sigma} - \Sigma_{\sigma\bar{\sigma}} \tilde{G}_{\bar{\sigma}\bar{\sigma}}^{0} \Sigma_{\bar{\sigma}\sigma}]^{-1} & \tilde{G}_{\sigma\sigma}^{0} \Sigma_{\sigma\bar{\sigma}} G_{\bar{\sigma}\bar{\sigma}} \\ \tilde{G}_{\bar{\sigma}\bar{\sigma}}^{0} \Sigma_{\bar{\sigma}\sigma} G_{\sigma\sigma} & [(G_{\bar{\sigma}\bar{\sigma}}^{0})^{-1} - \Sigma_{\bar{\sigma}\bar{\sigma}} - \Sigma_{\bar{\sigma}\sigma} \tilde{G}_{\sigma\sigma}^{0} \Sigma_{\sigma\bar{\sigma}}]^{-1} \end{bmatrix} \tag{2}$$

where the self-energy $\Sigma_{\sigma\sigma}$ is caused by tunneling without an associated spin flip and the self-energy $\Sigma_{\bar{\sigma}\sigma}$ is caused by spin-flip-associated tunneling. $\Sigma_{\bar{\sigma}\sigma}$ flips spin σ to spin $\bar{\sigma}$ during the electron transport between the lead and the dot. $G_{\sigma\sigma}^{0}$ is the free-particle Green's function and $\tilde{G}_{\sigma\sigma}^{0} = (\omega - \epsilon_{\sigma} - \Sigma_{\sigma\sigma})^{-1}$ is the Green's function of the electron in the QD with the spin state σ perturbed by the tunneling effect. The detailed derivation of Eq. (2) is shown in Appendix A.

If the intradot Coulomb interaction is included, the Kondo effect occurs when $T \leqslant T_K$. There are many approaches to solve the problem, such as the noncrossing-approximation approach,[18,11] the equation of motion (EOM) method,[19–22,10] or the renormalization group method.[12,20,23] The equation of motion method will be used to solve the Green's function of the interaction system in this work. In the processes of the EOM, the two-particle correlation function (or Green's function) arises from the two-particle on-site Coulomb interaction and needs to be decoupled. The accuracy of the EOM method depends on the decoupling scheme. One of the compact ways to decouple the two-particle correlation function to the single-particle correlation function is the decoupling scheme introduced by Lacroix for high temperature

(i.e., $T \geqslant T_K$). The high-temperature Lacroix decoupling approximation at low temperatures ($T < T_K$) gives only a qualitative solution and is quantitatively correct at high temperatures ($T \geqslant T_K$).[9,20] The EOM and Lacroix's high-temperature decoupling scheme are popularly adopted by many authors. In this work, we will use the high-temperature Lacroix decoupling approximation to decouple the two-particle Green's function.

Consider the spin-flip-associated tunneling effect where the intradot particle-particle interaction is assumed to be the Coulomb interaction. By using the method of the equation of motion in the Green's function $\mathbf{G}$, one obtains

$$\begin{bmatrix} (\omega-\epsilon_\sigma)G_{\sigma\sigma} & (\omega-\epsilon_\sigma)G_{\sigma\bar{\sigma}} \\ (\omega-\epsilon_{\bar{\sigma}})G_{\bar{\sigma}\sigma} & (\omega-\epsilon_{\bar{\sigma}})G_{\bar{\sigma}\bar{\sigma}} \end{bmatrix} = \begin{bmatrix} 1 & 0 \\ 0 & 1 \end{bmatrix} + \begin{bmatrix} \Sigma^{Tn}_{\sigma\sigma} & \Sigma^{Ts}_{\sigma\bar{\sigma}} \\ \Sigma^{Ts}_{\bar{\sigma}\sigma} & \Sigma^{Tn}_{\bar{\sigma}\bar{\sigma}} \end{bmatrix} \begin{bmatrix} G_{\sigma\sigma} & G_{\sigma\bar{\sigma}} \\ G_{\bar{\sigma}\sigma} & G_{\bar{\sigma}\bar{\sigma}} \end{bmatrix} + U \begin{bmatrix} G^{(2)}_{\sigma\sigma} & G^{(2)}_{\sigma\bar{\sigma}} \\ G^{(2)}_{\bar{\sigma}\sigma} & G^{(2)}_{\bar{\sigma}\bar{\sigma}} \end{bmatrix} \tag{3}$$

where $G_{\sigma\sigma'} \equiv (-i)\langle T\{d_\sigma, d^\dagger_{\sigma'}\}\rangle$ and $G^{(2)}_{\sigma\sigma'} \equiv (-i)\langle T\{d_\sigma n_{\bar{\sigma}}, d^\dagger_{\sigma'}\}\rangle$. The Green's function $G^{(2)}_{\sigma\sigma'}$ is the two-particle Green's function corresponding to particle-particle interaction (Coulomb interaction) and is related to the Kondo effect. Using the EOM in $\mathbf{G}^{(2)}$, we obtain

$$\begin{aligned} \begin{bmatrix} (\omega-\epsilon_\sigma-U)G^{(2)}_{\sigma\sigma} & (\omega-\epsilon_\sigma-U)G^{(2)}_{\sigma\bar{\sigma}} \\ (\omega-\epsilon_{\bar{\sigma}}-U)G^{(2)}_{\bar{\sigma}\sigma} & (\omega-\epsilon_{\bar{\sigma}}-U)G^{(2)}_{\bar{\sigma}\bar{\sigma}} \end{bmatrix} &= \begin{bmatrix} \langle n_{\bar{\sigma}}\rangle & 0 \\ 0 & \langle n_\sigma\rangle \end{bmatrix} + \sum_{k_\alpha s} \begin{bmatrix} V^*_{k\alpha s,\sigma}(-i)\langle T\{c_{k_\alpha s}d^\dagger_{\bar{\sigma}}d_{\bar{\sigma}}, d^\dagger_\sigma\}\rangle & V^*_{k\alpha s,\sigma}(-i)\langle T\{c_{k_\alpha s}d^\dagger_{\bar{\sigma}}d_{\bar{\sigma}}, d^\dagger_{\bar{\sigma}}\}\rangle \\ V^*_{k\alpha s,\bar{\sigma}}(-i)\langle T\{c_{k_\alpha s}d^\dagger_{\sigma}d_{\sigma}, d^\dagger_\sigma\}\rangle & V^*_{k\alpha s,\bar{\sigma}}(-i)\langle T\{c_{k_\alpha s}d^\dagger_{\sigma}d_{\sigma}, d^\dagger_{\bar{\sigma}}\}\rangle \end{bmatrix} \\ &\quad + \sum_{k_\alpha s} \begin{bmatrix} V_{k\alpha s,\bar{\sigma}}(-i)\langle T\{c^\dagger_{k_\alpha s}d_\sigma d_{\bar{\sigma}}, d^\dagger_\sigma\}\rangle & V_{k\alpha s,\bar{\sigma}}(-i)\langle T\{c^\dagger_{k_\alpha s}d_\sigma d_{\bar{\sigma}}, d^\dagger_{\bar{\sigma}}\}\rangle \\ V_{k\alpha s,\sigma}(-i)\langle T\{c^\dagger_{k_\alpha s}d_{\bar{\sigma}} d_{\sigma}, d^\dagger_\sigma\}\rangle & V_{k\alpha s,\sigma}(-i)\langle T\{c^\dagger_{k_\alpha s}d_{\bar{\sigma}} d_{\sigma}, d^\dagger_{\bar{\sigma}}\}\rangle \end{bmatrix} \\ &\quad - \sum_{k_\alpha s} \begin{bmatrix} V^*_{k\alpha s,\bar{\sigma}}(-i)\langle T\{c_{k_\alpha s}d^\dagger_{\bar{\sigma}}d_{\sigma}, d^\dagger_\sigma\}\rangle & V^*_{k\alpha s,\bar{\sigma}}(-i)\langle T\{c_{k_\alpha s}d^\dagger_{\bar{\sigma}}d_{\sigma}, d^\dagger_{\bar{\sigma}}\}\rangle \\ V^*_{k\alpha s,\sigma}(-i)\langle T\{c_{k_\alpha s}d^\dagger_{\sigma}d_{\bar{\sigma}}, d^\dagger_\sigma\}\rangle & V^*_{k\alpha s,\sigma}(-i)\langle T\{c_{k_\alpha s}d^\dagger_{\sigma}d_{\bar{\sigma}}, d^\dagger_{\bar{\sigma}}\}\rangle \end{bmatrix}. \end{aligned} \tag{4}$$

In general there are four one-particle Green's functions ($G_{\sigma\sigma}$, $G_{\sigma\bar{\sigma}}$, $G_{\bar{\sigma}\sigma}$, and $G_{\bar{\sigma}\bar{\sigma}}$) and four two-particle Green's functions ($G^{(2)}_{\sigma\sigma}$, $G^{(2)}_{\sigma\bar{\sigma}}$, $G^{(2)}_{\bar{\sigma}\sigma}$, and $G^{(2)}_{\bar{\sigma}\bar{\sigma}}$) in our system. In contrast with Eq. (3), the equation of the Green's function $\mathbf{G}^{(2)}$ can be assumed as

$$\begin{aligned} &\begin{bmatrix} (\omega-\epsilon_\sigma-U)G^{(2)}_{\sigma\sigma} & (\omega-\epsilon_\sigma-U)G^{(2)}_{\sigma\bar{\sigma}} \\ (\omega-\epsilon_{\bar{\sigma}}-U)G^{(2)}_{\bar{\sigma}\sigma} & (\omega-\epsilon_{\bar{\sigma}}-U)G^{(2)}_{\bar{\sigma}\bar{\sigma}} \end{bmatrix} \\ &\quad = \begin{bmatrix} \langle n_{\bar{\sigma}}\rangle & 0 \\ 0 & \langle n_\sigma\rangle \end{bmatrix} + \begin{bmatrix} X^{(2)}_{\sigma\sigma} & X^{(2)}_{\sigma\bar{\sigma}} \\ X^{(2)}_{\bar{\sigma}\sigma} & X^{(2)}_{\bar{\sigma}\bar{\sigma}} \end{bmatrix} \begin{bmatrix} G_{\sigma\sigma} & G_{\sigma\bar{\sigma}} \\ G_{\bar{\sigma}\sigma} & G_{\bar{\sigma}\bar{\sigma}} \end{bmatrix} \\ &\quad + \begin{bmatrix} Y^{(2)}_{\sigma\sigma} & Y^{(2)}_{\sigma\bar{\sigma}} \\ Y^{(2)}_{\bar{\sigma}\sigma} & Y^{(2)}_{\bar{\sigma}\bar{\sigma}} \end{bmatrix} \begin{bmatrix} G^{(2)}_{\sigma\sigma} & G^{(2)}_{\sigma\bar{\sigma}} \\ G^{(2)}_{\bar{\sigma}\sigma} & G^{(2)}_{\bar{\sigma}\bar{\sigma}} \end{bmatrix}. \end{aligned} \tag{5}$$

In order to simplify the problem, we consider the infinite-U limit. Under the infinite-U limit, the off-diagonal term of $\mathbf{Y}^{(2)}$ can be ignored (the detailed derivation will be given in Appendix B). Equation (5) can be rewritten as

$$\begin{aligned} &\begin{bmatrix} G^{(2)}_{\sigma\sigma} & G^{(2)}_{\sigma\bar{\sigma}} \\ G^{(2)}_{\bar{\sigma}\sigma} & G^{(2)}_{\bar{\sigma}\bar{\sigma}} \end{bmatrix} \\ &\quad = \begin{bmatrix} g^{0(2)}_{\sigma\sigma}\langle n_{\bar{\sigma}}\rangle & 0 \\ 0 & g^{0(2)}_{\sigma\sigma}\langle n_\sigma\rangle \end{bmatrix} \\ &\quad + \begin{bmatrix} g^{0(2)}_{\sigma\sigma}(X^{(2)}_{\sigma\sigma}G_{\sigma\sigma} + X^{(2)}_{\sigma\bar{\sigma}}G_{\bar{\sigma}\sigma}) & g^{0(2)}_{\sigma\sigma}(X^{(2)}_{\sigma\bar{\sigma}}G_{\bar{\sigma}\bar{\sigma}} + X^{(2)}_{\sigma\sigma}G_{\sigma\bar{\sigma}}) \\ g^{0(2)}_{\bar{\sigma}\bar{\sigma}}(X^{(2)}_{\bar{\sigma}\sigma}G_{\sigma\sigma} + X^{(2)}_{\bar{\sigma}\bar{\sigma}}G_{\bar{\sigma}\sigma}) & g^{0(2)}_{\bar{\sigma}\bar{\sigma}}(X^{(2)}_{\bar{\sigma}\sigma}G_{\sigma\bar{\sigma}} + X^{(2)}_{\bar{\sigma}\bar{\sigma}}G_{\bar{\sigma}\bar{\sigma}}) \end{bmatrix} \end{aligned}$$

where $g^{0(2)}_{\sigma\sigma} \equiv (\omega-\epsilon_\sigma-Y_{\sigma\sigma}-U)^{-1}$ and $g^{0(2)}_{\bar{\sigma}\bar{\sigma}} \equiv (\omega-\epsilon_{\bar{\sigma}}-Y_{\bar{\sigma}\bar{\sigma}}-U)^{-1}$. Substituting $\mathbf{G}^{(2)}$ into $\mathbf{G}$, one obtains

$$\begin{aligned} \begin{bmatrix} (\omega-\epsilon_\sigma)G_{\sigma\sigma} & (\omega-\epsilon_\sigma)G_{\sigma\bar{\sigma}} \\ (\omega-\epsilon_{\bar{\sigma}})G_{\bar{\sigma}\sigma} & (\omega-\epsilon_{\bar{\sigma}})G_{\bar{\sigma}\bar{\sigma}} \end{bmatrix} &= \begin{bmatrix} 1+Ug^{0(2)}_{\sigma\sigma}\langle n_{\bar{\sigma}}\rangle & 0 \\ 0 & 1+Ug^{0(2)}_{\bar{\sigma}\bar{\sigma}}\langle n_\sigma\rangle \end{bmatrix} + \begin{bmatrix} \Sigma^T_{\sigma\sigma}+Ug^{0(2)}_{\sigma\sigma}X^{(2)}_{\sigma\sigma} & \Sigma^T_{\sigma\bar{\sigma}}+Ug^{0(2)}_{\sigma\sigma}X^{(2)}_{\sigma\bar{\sigma}} \\ \Sigma^T_{\bar{\sigma}\sigma}+Ug^{0(2)}_{\bar{\sigma}\bar{\sigma}}X^{(2)}_{\bar{\sigma}\sigma} & \Sigma^T_{\bar{\sigma}\bar{\sigma}}+Ug^{0(2)}_{\bar{\sigma}\bar{\sigma}}X^{(2)}_{\bar{\sigma}\bar{\sigma}} \end{bmatrix} \begin{bmatrix} G_{\sigma\sigma} & G_{\sigma\bar{\sigma}} \\ G_{\bar{\sigma}\sigma} & G_{\bar{\sigma}\bar{\sigma}} \end{bmatrix} \\ &\equiv \begin{bmatrix} 1+Ug^{0(2)}_{\sigma\sigma}\langle n_{\bar{\sigma}}\rangle & 0 \\ 0 & 1+Ug^{0(2)}_{\bar{\sigma}\bar{\sigma}}\langle n_\sigma\rangle \end{bmatrix} + \begin{bmatrix} \Sigma^{tot}_{\sigma\sigma} & \Sigma^{tot}_{\sigma\bar{\sigma}} \\ \Sigma^{tot}_{\bar{\sigma}\sigma} & \Sigma^{tot}_{\bar{\sigma}\bar{\sigma}} \end{bmatrix} \begin{bmatrix} G_{\sigma\sigma} & G_{\sigma\bar{\sigma}} \\ G_{\bar{\sigma}\sigma} & G_{\bar{\sigma}\bar{\sigma}} \end{bmatrix}. \end{aligned}$$

Under the infinite-U limit, $U\mathbf{g}^{0(2)} \sim -1$ and $\mathbf{\Sigma}^{tot} = \mathbf{\Sigma}^T - \mathbf{X}^{(2)}$. Comparing to Eq. (2) (after some algebra), one obtains

$$\begin{bmatrix} G_{\sigma\sigma} & G_{\sigma\bar{\sigma}} \\ G_{\bar{\sigma}\sigma} & G_{\bar{\sigma}\bar{\sigma}} \end{bmatrix} = \begin{bmatrix} (1-\langle n_{\bar{\sigma}}\rangle)[(\tilde{G}^0_{\sigma\sigma})^{-1} - \Sigma^{tot}_{\sigma\bar{\sigma}}\tilde{G}^0_{\bar{\sigma}\bar{\sigma}}\Sigma^{tot}_{\bar{\sigma}\sigma}]^{-1} & \tilde{G}^0_{\sigma\sigma}\Sigma^{tot}_{\sigma\bar{\sigma}}G_{\bar{\sigma}\bar{\sigma}} \\ \tilde{G}^0_{\bar{\sigma}\bar{\sigma}}\Sigma^{tot}_{\bar{\sigma}\sigma}G_{\sigma\sigma} & (1-\langle n_{\sigma}\rangle)[(\tilde{G}^0_{\bar{\sigma}\bar{\sigma}})^{-1} - \Sigma^{tot}_{\bar{\sigma}\sigma}\tilde{G}^0_{\sigma\sigma}\Sigma^{tot}_{\sigma\sigma'}]^{-1} \end{bmatrix}. \quad (6)$$

In Eq. (6) $\tilde{G}^0_{\sigma\sigma} \equiv (\omega - \epsilon_\sigma - \Sigma^{tot}_{\sigma\sigma})^{-1}$ and $\tilde{G}^0_{\bar{\sigma}\bar{\sigma}} \equiv (\omega - \epsilon_{\bar{\sigma}} - \Sigma^{tot}_{\bar{\sigma}\bar{\sigma}})^{-1}$. Comparing $\tilde{G}^0_{\sigma\sigma}$ with Eq. (3) in Ref. 20,

$$G_{\sigma\sigma} = \frac{1-\langle n_{\bar{\sigma}}\rangle}{\omega - \epsilon_\sigma - \Sigma_{0\sigma} - \Sigma_{1\sigma}}, \quad (7)$$

which is the Green's function corresponding to the original Anderson model. Now set $\mathbf{X}^{(2)} \equiv -\mathbf{\Sigma}_{1\sigma}$. $\tilde{\mathbf{G}}^0$ is the same as the Green's function corresponding to the original Anderson Hamiltonian except for the factor $(1-\langle n_{\bar{\sigma}}\rangle)$. $\tilde{\mathbf{G}}^0$ can be regarded as the Green's function of the quasiparticle of the Anderson Hamiltonian without the spin-flip effect. Now, the remaining problem is to obtain $\mathbf{X}^{(2)}$ and $\mathbf{Y}^{(2)}$. The detailed derivation and results are presented in Appendix B.

The form of our result [Eq. (6)] is the same as Eq. (2) except for the self-energy $\mathbf{X}^{(2)}$ which is related to the Kondo effect. The physical picture of the Green's function [Eq. (6)] can be interpreted as follows. $\tilde{\mathbf{G}}^0$ is the Green's function corresponding to the Anderson Hamiltonian without the spin-flip effect, i.e., it is the form of the Green's function as shown in Eq. (3) of Ref. 20. $G_{\sigma\sigma}$ in Eq. (6), for example, represents the corresponding σ-state quasiparticle of the Anderson Hamiltonian, which is scattered between the σ and $\bar{\sigma}$ states and causes the self-energy $\Sigma^{tot}_{\sigma\bar{\sigma}}\tilde{G}^0_{\bar{\sigma}\bar{\sigma}}\Sigma^{tot}_{\bar{\sigma}\sigma}$. $\Sigma^{tot}_{\bar{\sigma}\sigma}$ contains two terms: the self-energy $\Sigma^T_{\bar{\sigma}\sigma}$ corresponding to the scattering via the normal channel and the self-energy $X^{(2)}_{\bar{\sigma}\sigma}$ corresponding to the scattering via the Kondo channel. The normal-channel scattering is energy and temperature independent. Since the Kondo effect is strongly dependent on the temperature and causes a Kondo resonant peak in the vicinity of the Fermi level of the lead, the Kondo-channel scattering is strongly dependent on the temperature and dominates the scattering with energy in the vicinity of the Fermi energy of the lead.

Since the transport problem in a quantum dot system may be a nonequilibrium problem, we will employ the nonequilibrium Green's function method and the transport equation developed by Wingreen *et al.* to calculate the particle number and conductance.[25] To evaluate Eq. (6) numerically, one must determine the particle number $\langle n_\sigma\rangle$ and the expectation value $\langle d^\dagger_\sigma d_{\bar{\sigma}}\rangle$ by a self-consistent method. In order to calculate the expectation values $\langle n_\sigma\rangle$ and $\langle d^\dagger_\sigma d_{\bar{\sigma}}\rangle$, the corresponding lesser Green's functions $G^<_{\sigma\sigma}$ and $G^<_{\bar{\sigma}\sigma}$ must be solved first, i.e., $\langle n_\sigma\rangle = -i\int(d\epsilon/2\pi)G^<_{\sigma\sigma}$ and $\langle d^\dagger_\sigma d_{\bar{\sigma}}\rangle = -i\int(d\epsilon/2\pi)G^<_{\bar{\sigma}\sigma}$. In this work, we use the method proposed by Sun and Guo which is able to solve the lesser Green's function, of the interacting system exactly for the steady-state problem.[24] The detailed derivation processes are shown in Appendix C.

III. RESULTS AND DISCUSSION

In the following discussion, all energy scales are normalized to the normal-tunneling coupling constant $\Gamma^n_\alpha = 1$. The resonant energy of the quantum dot is set as $\epsilon_0 = -5$. The Fermi level of the lead E_F is set to be zero for the equilibrium situation. The temperature is normalized to the Kondo temperature T_K, which is calculated by the exact expression obtained by Haldane, $T_K \approx (D\Gamma)^{1/2}\exp[\pi(\epsilon_0 - E_F)/(2\Gamma)] \approx 0.004$,[26] with the half-width $D = 100$ and $\Gamma = \Gamma^n_L + \Gamma^n_R$.

Since the high temperature Lacroix decoupling approximation at low temperatures ($T < T_K$) gives only a qualitative solution and is quantitatively correct at high temperatures ($T > T_K$), we consider the situation with the temperature near the Kondo temperature, i.e., $T = 10T_K$, $1T_K$, and $0.1T_K$, and the normal limit $T = 100T_K$, for which the Kondo effect can be ignored for comparison.[27] The spectral function $A_{\sigma'\sigma}(\omega) = -2\,\mathrm{Im}\,G^r_{\sigma'\sigma}$ (or local density of states when $\sigma' = \sigma$) in the equilibrium situation is calculated in terms of the strength of spin-flip-associated tunneling, which is described by the spin-flip coupling constant Γ^s. As in the previous discussion, the quasiparticle of the Anderson Hamiltonian is scattered by the normal and the Kondo channels. The self-energy $\mathbf{\Sigma}^T$ due to normal-channel scattering is independent of the energy and the temperature; thus the electron can be scattered by the normal channel at arbitrary energy and temperature. In contrast to the normal channel, the Kondo-effect channel is energy dependent and the strength increases logarithmically in the vicinity of the Fermi level when $T \leqslant T_K$. Thus, the self-energy corresponding to the Kondo channel $\mathbf{X}^{(2)}$ is sensitive to temperature and energy. It can be expected that the Kondo channel dominates the scattering due to spin-flip-associated tunneling in the vicinity of the Fermi level when $T \leqslant T_K$. The normal-channel scattering dominates the spin-flip effect for electrons with energies far away from the Fermi level or $T > T_K$. As shown in Fig. 2, the LDOS in the region far away from the Fermi level is temperature independent. It implies that an electron with energy far away from the Fermi level is mainly scattered by the normal channel. Figure 3 shows a detailed plot of the LDOS with energy in the vicinity of the Fermi level. The spectral functions for $T = 100T_K$, i.e., the normal case, are shown in Figs. 3(a) and 3(b) (dashed lines). The spin-flip scattering via the normal channel affects the diagonal part of the spectrum function $A_{\sigma\sigma}$ (or LDOS) very slightly for the case of $T = 100T_K$ (normal limit). But the dependence of the off-diagonal spectrum function $A_{\bar{\sigma}\sigma}$ on spin-flip scattering via the classical channel is stronger than for $A_{\sigma\sigma}$. When the temperature is decreased to the order of the Kondo temperature ($T = 10T_K$ and $1T_K$ in our case), the Kondo effect becomes obvious and the Kondo resonance peak grows logarithmically. As Figs. 3(a) and 3(b) (solid line) and Figs. 3(c) and 3(d) show, it is obvious that the

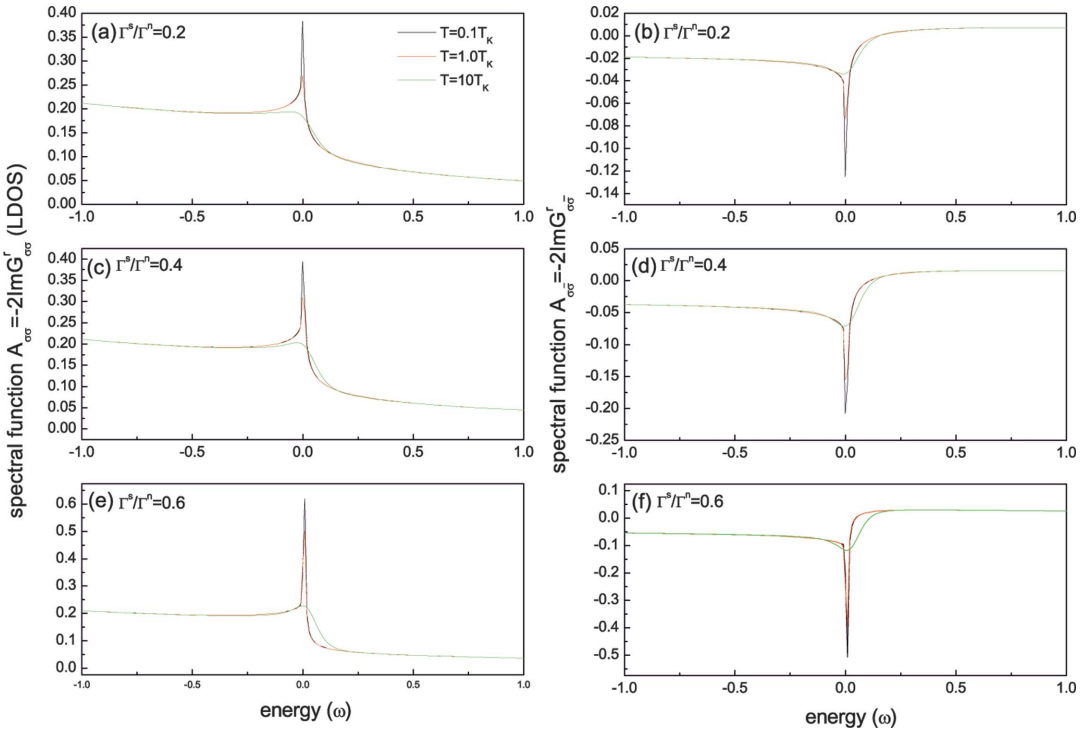

FIG. 2. (Color) The plot of spectral function as a function of ω with temperature $T=10T_K$, $1T_K$, and $T=0.1T$.

LDOS with energy near the Fermi level is strongly dependent on temperature when the temperature is close to the Kondo temperature. Therefore, it implies that the scattering in the region near the Fermi level is dominated by the Kondo channel. When the temperature is below the Kondo temperature ($T=0.1T_K$ in our case), the scattering via the Kondo channel is prominent. As shown in Figs. 3(e) and 3(f), there are two major effects due to the spin-flip-associated tunneling via the Kondo channel. The amplitude of the Kondo resonance peak is increased as Γ^s is increased, i.e., the

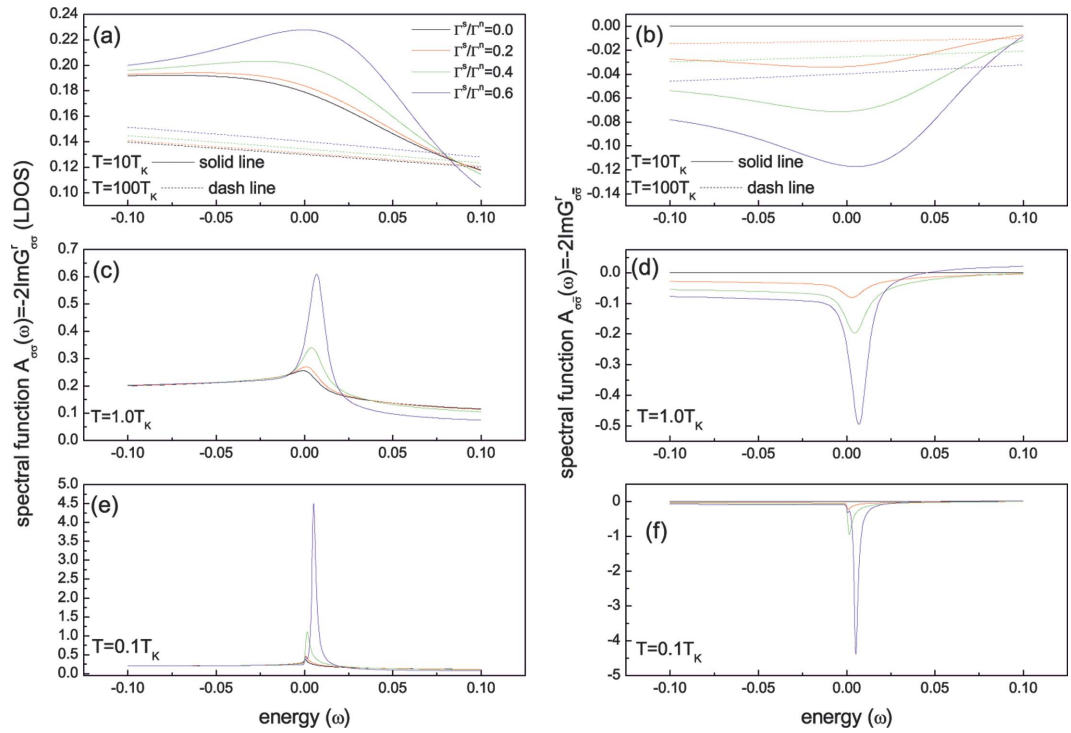

FIG. 3. (Color) The detailed plot of the spectral function in the vicinity of the Fermi level as a function of ω. $T=$(a)$100T_K$ and $10T_K$, (b) $1T_K$, and (c) $0.1T_K$ with various $\Gamma^s_\alpha/\Gamma^n_\alpha$.

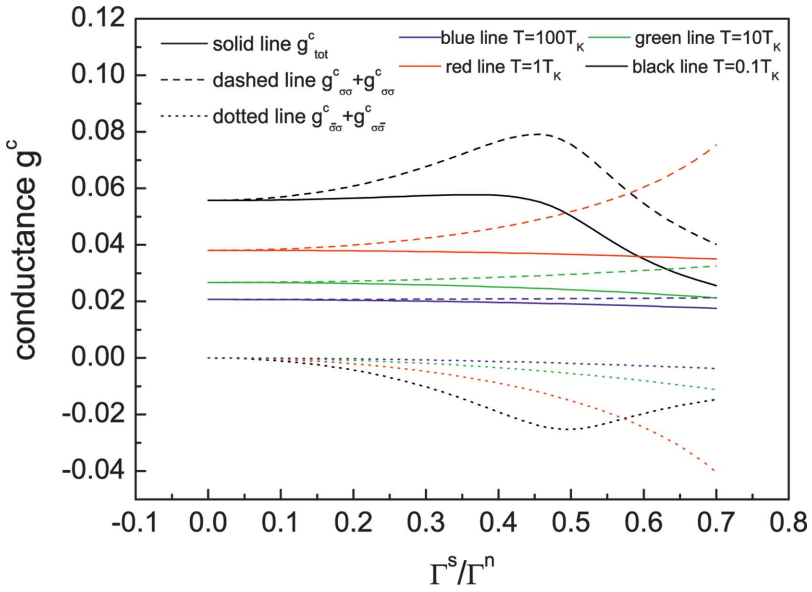

FIG. 4. (Color) The equilibrium conductance versus $\Gamma^s_\alpha/\Gamma^n_\alpha$ at various temperatures. The dashed line is the diagonal part. The dotted line is the off-diagonal part. The solid line is the total conductance. The blue line is $T=100T_K$, the green line $T=10T_K$, the red line is $T=1T_K$, and the black line is $T=0.1T_K$

Kondo resonance peak is enhanced by the spin-flip-associated tunneling effect. In addition to the increasing of the peak height, the spin-flip tunneling also causes a blue-shift of the Kondo resonance. These effects become stronger as the temperature is decreased. Note that the enhancement and shift of the Kondo resonance peak due to spin-flip-associated tunneling will affect the conductance. Since the off-diagonal Green's function is $G_{\bar{\sigma}\sigma}=\tilde{G}^0_{\sigma\sigma}\Sigma^{tot}_{\bar{\sigma}\sigma}G_{\sigma\sigma}$, the profile of the off-diagonal spectral function $A_{\bar{\sigma}\sigma}$ is similar to that of the diagonal spectral function $A_{\sigma\sigma}$ but with opposite sign. It is worth noting that for the case of $T \geqslant T_K$, the decrease (to more negative values) of $A_{\bar{\sigma}\sigma}$ is faster than the increase of $A_{\sigma\sigma}$. This phenomenon is the main reason for suppression of the conductance for $T \geqslant T_K$.

The conductance g^c for the equilibrium case is calculated by Eq. (3) of Ref. 13. For the equilibrium situation, the current is contributed by the electrons with energy near the Fermi level of the leads. Thus, the equilibrium conductance reflects the properties of the Kondo resonance peak with energy in the vicinity of the Fermi level of the leads. Figure 4 shows the equilibrium conductance versus the spin-flip coupling constant Γ^s. One can find that for $\Gamma^s=0$, the total conductance g^c_{tot} is increased as the temperature is decreased, since the Kondo resonance peak is enhanced as the temperature is decreased. For the case of $T=100T_K$, the Kondo effect can be ignored and the scattering is dominated by the normal channel. As in previous discussion, the decrease of $A_{\bar{\sigma}\sigma}$ is faster than the increase of $A_{\sigma\sigma}$ as Γ^s is increased; hence the total conductance g^c_{tot} is dominated by the off-diagonal part conductance $g^c_{\sigma\bar{\sigma}}$ and decreased as Γ^s is increased. For the cases of $T=10T_K$ and $1.0T_K$ the Kondo effect appears; however, it is not obvious. One can find that $g^c_{\sigma\sigma}$ is increased slightly as Γ^s is increased for $\Gamma^s > 0.3\Gamma^n(0.1\Gamma^n)$. This phenomenon reflects the enhancement of the Kondo resonance peak due to the spin-flip effect via the Kondo channel as discussed previously. Similar to the case of $T=100T_K$, the total conductance is dominated by the off-diagonal conductance and decreased as Γ^s is increased. For the case of $T=0.1T_K$, the effect due to spin-flip scattering via the Kondo channel becomes more prominent. The diagonal part $g^c_{\sigma\sigma}$ contains peak-enhancement and peak-shift effects due to spin-flip via the Kondo channel. For $\Gamma^s < 0.48$, the peak-enhancement effect is dominant and $g^c_{\sigma\sigma}$ increases as Γ^s is increased. For $\Gamma^s > 0.48$, the peak-shift effect is dominant and thus the peak height is shifted out of the vicinity of the Fermi level of the leads, and thus there are fewer electrons contributing to the conductance; hence $g^c_{\sigma\sigma}$ is decreased. The profile of the off-diagonal spectral function $A_{\bar{\sigma}\sigma}$ is similar to that of $A_{\sigma\sigma}$ except with the opposite sign; thus the behavior of the off-diagonal part of the conductance is similar to the diagonal part except for the sign. For $T=0.1T_K$ the total conductance is dominated by $g^c_{\sigma\sigma}$. In the region dominated by the peak-enhancement effect, i.e., $\Gamma^s < 0.48$, the total conductance is slightly increased as Γ^s is increased. In the region dominated by the peak-shift effect, the total conductance decreases as Γ^s is increased. Note that the conductance is suppressed rapidly for the case of $T=0.1T_K$ when $\Gamma^s > 0.48$. The rapid decrease of conductance is caused by the peak-shift effect due to spin-flip scattering.

For the nonequilibrium case, a quantum dot connected to two leads with different Fermi levels is studied. The Fermi levels of leads are set to be zero when the bias voltage is zero. When the bias voltage V_{bias} is applied, the Fermi levels of the leads are $E^R_F=-V_{bias}/2$ and $E^L_F=V_{bias}/2$. The nonequilibrium differential conductance is defined as $g^c=\Delta J/\Delta V_{bias}$, where the current J is calculated by the method of Ref. 25. The nonequilibrium differential conductance is shown in Fig. 5. Since the applied bias is symmetry, the conductance is symmetry for $V_{bias}>0$ and $V_{bias}<0$, as shown in Figs. 5(a) and 5(b). Following the same reasoning, the nonequilibrium differential conductance is decreased as Γ_s is increased for the cases of $T \geqslant T_K$. In the region $|V_{bias}|>0.25$ the conductance is temperature insensitive. It implies that the nonequilibrium differential conductance for $|V_{bias}|>0.25$ is dominated by the scattering via the normal channel, the behavior of the differential conductance is similar to the equilibrium case for $T > T_K$. Hence, for $|V_{bias}|>0.25$, the differential conductance is decreased as Γ^s is increased. In the region with energy near the Fermi level, i.e., $|V_{bias}|<0.25$, the Kondo

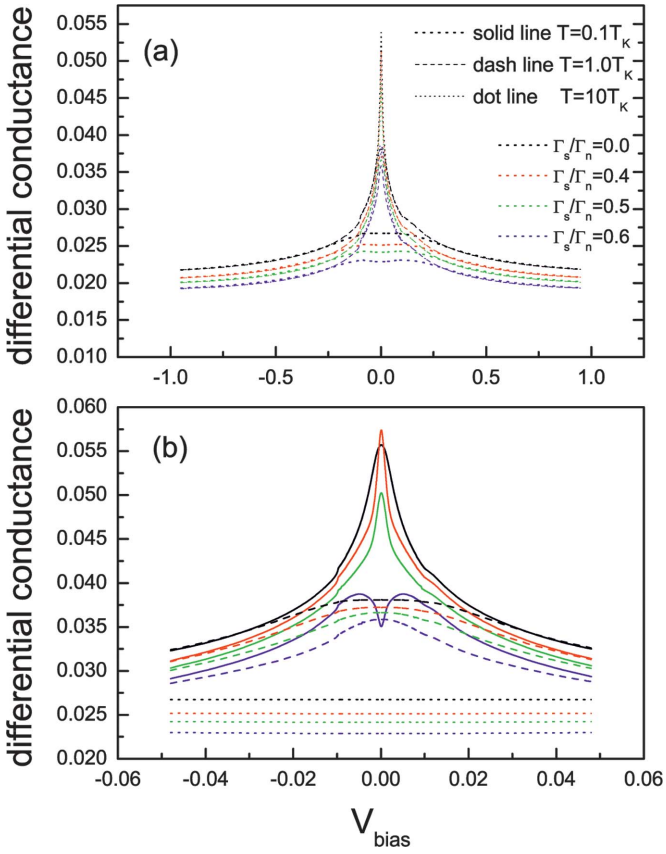

FIG. 5. (Color) (a) The differential conductance versus bias voltage with various $\Gamma^s_\alpha/\Gamma^n_\alpha$ for different temperature. (b) A detailed plot of (a) with energy almost equal to zero bias voltage.

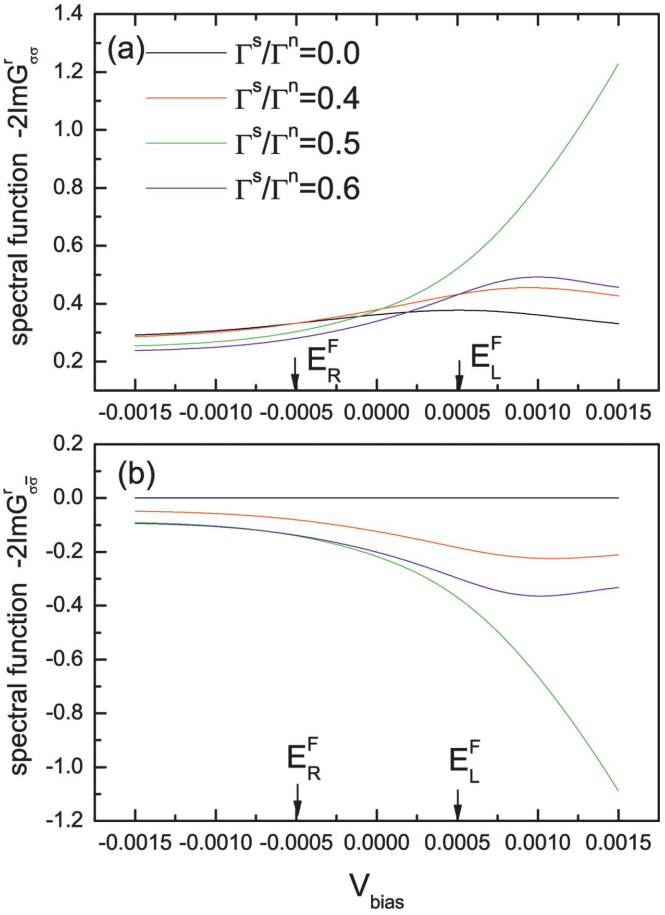

FIG. 6. (Color) (a) The nonequilibrium diagonal and (b) off-diagonal spectral functions for the case of $V_{bias}=10^{-3}$ and $T=0.1T_K$ with various $\Gamma^s_\alpha/\Gamma^n_\alpha$.

effect is more important when $T<T_k$. This is because the Kondo effect influences the LDOS only when the electron energy is near the Fermi level. The nonequilibrium differential conductance is influenced strongly by the Kondo effect when the bias voltage $|V_{bias}|\sim 0$ for $T\leqslant T_k$. Figure 5(b) shows a detailed plot of the nonequilibrium differential conductance with bias voltage $|V_{bias}|<0.05$. The variation of the conductance for $|V_{bias}|\sim 0$ is similar to the case of $|V_{bias}|\gg 0$ when $T>T_k$ (the dotted line in Fig. 5) and the scattering is via the normal channel. As the temperature is decreased to $T\sim T_k$, the influence due to the Kondo effect becomes important and the Kondo resonance peak is prominent. Hence, the conductance is larger than the one for $T>T_k$. For $T=T_k$ (the dashed line in Fig. 5), the quantity of conductance suppression due to the spin-flip-associated tunneling is similar to that in the large-bias-voltage region. The suppression of conductance is due to the decrease of $g^c_{\sigma\bar{\sigma}}$ as Γ^s is increased. The prominence of the conductance reflects the prominent Kondo resonance peak of the LDOS. When $T\leqslant T_k$ (the solid line in Fig. 5), the influence of the peak shift of the Kondo resonance becomes important. As in the case of equilibrium, the $g^c_{\sigma\sigma}$ is strongly suppressed by the shift of the Kondo resonance peak when Γ_s is large. As a result, the total conductance is suppressed rapidly when $\Gamma^s>0.4$ and causes a valley when $\Gamma^s=0.6$. Figures 6(a) and 6(b) show the spectral function for $T=0.1T_K$ and $V_{bias}=10^{-3}$. One can find that the LDOS within the Fermi level of the leads is increased as Γ^s is increased when $\Gamma^s<0.6$. This explains why the differential conductance is increased as Γ^s is increased when $\Gamma^s<0.6$ and $T=0.1T_K$ in the vicinity of $V_{bias}=0$. For $\Gamma^s=0.6$, the peak-shift effect shifts the peak height out of the region between the Fermi level of the leads and the total LDOS within the Fermi level of the leads is smaller than the LDOS for $\Gamma^s<0.6$. Hence, the differential conductance appears slightly when $V_{bias}\sim 0$ for $T=0.1T_K$ and $\Gamma^s=0.6$. This tip of the conductance occurs when $T<T_k$ in the vicinity of the Fermi level of the leads, therefore, this phenomenon mainly originates from the scattering via the Kondo channel.

IV. SUMMARY

In summary, we study the spin-flip-associated tunneling in the Anderson model. The total effect can be interpreted as follows. As Eq. (6) shows, the quasiparticle described by the Anderson Hamiltonian is scattered via the normal and the Kondo channels. The normal channel dominates the scattering of the electrons with energy far away from the Fermi level of the lead. The electrons with energy near the Fermi level of the leads are mainly scattered by the Kondo channel when $T\leqslant T_k$. Note that only the infinite-U limit approximation is used in Eq. (6), i.e., Eq. (6) is a general form for the

Anderson model with spin-flip-associated tunneling in the infinite-U limit and does not relate to the decoupling method. The spin-flip-associated tunneling via the Kondo channel causes two main effects. One is the enhancement of the Kondo resonance peak; the other is the blueshift of the Kondo resonance peak. When the temperature $T=10T_K$ and $1.0T_K$, the Kondo resonance peak is obviously enhanced by spin-flip-associated tunneling effect, but the blueshift of the Kondo resonance peak is not obvious. This effect is reflected in the conductance. The enhancement of the Kondo resonant peak causes an increase of the diagonal part of the conductance $g_{\sigma\sigma}$ and decreases the off-diagonal part of the conductance $g_{\bar{\sigma}\sigma}$ (to more negative values). Since the decrease of the off-diagonal part of the conductance is stronger than the increase of the diagonal part of the conductance; as a result the total conductance is suppressed by spin-flip-associated tunneling. The conductance due to off-diagonal processes is negative and cannot be neglected. As the temperature gets lower, the blueshift of the Kondo resonance peak becomes important. When $T \leqslant T_k$ and the spin-flip-associated coupling constant Γ_s is large enough, the blueshift of the Kondo resonance peak will cause a strong suppression of the diagonal part of the conductance and the total conductance is suppressed rapidly. The conductance suppression due to the shift of the Kondo resonance peak is ascribed to the Kondo channel mainly, since the effect occurs as $T<T_K$. The high-temperature Lacroix decoupling approximation is used to decouple the two-particle correlation function (or Green's function). Our result is quantitatively correct when $T>T_K$. The Kondo resonance peak is slightly enhanced and blueshifted as $T \geqslant T_K$. On the contrary, the Kondo resonance peak is enhanced prominently and blueshifted obviously in the case of $T=0.1T_k$. Although the decoupling approximation only gives a qualitative result for $T<T_K$, the conductance can be suppressed strongly by the spin-flip-associated tunneling effect for $T<T_K$.

ACKNOWLEDGMENT

This work is supported by the National Science Council of Taiwan under Grant No. NSC 94-2120-M-009-002.

APPENDIX A

First, we derive the general form of the Green's function for the spin-flip system. Assume that the lowest-order self-energies corresponding to the non-spin-flip transition processes $\sigma \to \sigma$ and $\bar{\sigma} \to \bar{\sigma}$ (the diagonal terms) are $\Sigma_{\sigma\sigma}$ and $\Sigma_{\bar{\sigma}\bar{\sigma}}$. And the lowest-order self-energies corresponding to the spin-flip transition processes $\bar{\sigma} \to \sigma$ and $\sigma \to \bar{\sigma}$ (the diagonal terms) are $\Sigma_{\sigma\bar{\sigma}}$ and $\Sigma_{\bar{\sigma}\sigma}$. The typical Dyson equation can be expressed as

$$\begin{bmatrix} G_{\sigma\sigma} & G_{\sigma\bar{\sigma}} \\ G_{\bar{\sigma}\sigma} & G_{\bar{\sigma}\bar{\sigma}} \end{bmatrix} = \begin{bmatrix} G^0_{\sigma\sigma} & 0 \\ 0 & G^0_{\bar{\sigma}\bar{\sigma}} \end{bmatrix} + \begin{bmatrix} G^0_{\sigma\sigma} & 0 \\ 0 & G^0_{\bar{\sigma}\bar{\sigma}} \end{bmatrix} \begin{bmatrix} \Sigma_{\sigma\sigma} & \Sigma_{\sigma\bar{\sigma}} \\ \Sigma_{\bar{\sigma}\sigma} & \Sigma_{\bar{\sigma}\bar{\sigma}} \end{bmatrix} \begin{bmatrix} G_{\sigma\sigma} & G_{\sigma\bar{\sigma}} \\ G_{\bar{\sigma}\sigma} & G_{\bar{\sigma}\bar{\sigma}} \end{bmatrix} = \begin{bmatrix} G^0_{\sigma\sigma} & 0 \\ 0 & G^0_{\bar{\sigma}\bar{\sigma}} \end{bmatrix} + \begin{bmatrix} G^0_{\sigma\sigma}\Sigma_{\sigma\sigma}G_{\sigma\sigma} + G^0_{\sigma\sigma}\Sigma_{\sigma\bar{\sigma}}G_{\bar{\sigma}\sigma} & G^0_{\sigma\sigma}\Sigma_{\sigma\sigma}G_{\sigma\bar{\sigma}} + G^0_{\sigma\sigma}\Sigma_{\sigma\bar{\sigma}}G_{\bar{\sigma}\bar{\sigma}} \\ G^0_{\bar{\sigma}\bar{\sigma}}\Sigma_{\bar{\sigma}\sigma}G_{\sigma\sigma} + G^0_{\bar{\sigma}\bar{\sigma}}\Sigma_{\bar{\sigma}\bar{\sigma}}G_{\bar{\sigma}\sigma} & G^0_{\bar{\sigma}\bar{\sigma}}\Sigma_{\bar{\sigma}\sigma}G_{\sigma\bar{\sigma}} + G^0_{\bar{\sigma}\bar{\sigma}}\Sigma_{\bar{\sigma}\bar{\sigma}}G_{\bar{\sigma}\bar{\sigma}} \end{bmatrix}. \tag{A1}$$

The off-diagonal terms can be rewritten as $G_{\sigma\bar{\sigma}}=\tilde{G}^0_{\sigma\sigma}\Sigma_{\sigma\bar{\sigma}}G_{\bar{\sigma}\bar{\sigma}}$ and $G_{\bar{\sigma}\sigma}=\tilde{G}^0_{\bar{\sigma}\bar{\sigma}}\Sigma_{\bar{\sigma}\sigma}G_{\sigma\sigma}$ where $\tilde{G}^0_{\sigma\sigma} \equiv [(G^0_{\sigma\sigma})^{-1}-\Sigma_{\sigma\sigma}]^{-1}$ and $\tilde{G}^0_{\bar{\sigma}\bar{\sigma}} \equiv [(G^0_{\bar{\sigma}\bar{\sigma}})^{-1}-\Sigma_{\bar{\sigma}\bar{\sigma}}]^{-1}$. Substitute these expressions for $G_{\sigma\bar{\sigma}}$ and $G_{\bar{\sigma}\sigma}$ into the diagonal term, Eq. (8) becomes

$$\begin{bmatrix} G_{\sigma\sigma} & G_{\sigma\bar{\sigma}} \\ G_{\bar{\sigma}\sigma} & G_{\bar{\sigma}\bar{\sigma}} \end{bmatrix} = \begin{bmatrix} [(G^0_{\sigma\sigma})^{-1} - \Sigma_{\sigma\sigma} - \Sigma_{\sigma\bar{\sigma}}\tilde{G}^0_{\bar{\sigma}\bar{\sigma}}\Sigma_{\bar{\sigma}\sigma}]^{-1} & G_{\sigma\bar{\sigma}} = \tilde{G}^0_{\sigma\sigma}\Sigma_{\sigma\bar{\sigma}}G_{\bar{\sigma}\bar{\sigma}} \\ \tilde{G}^0_{\bar{\sigma}\bar{\sigma}}\Sigma_{\bar{\sigma}\sigma}G_{\sigma\sigma} & [(G^0_{\bar{\sigma}\bar{\sigma}})^{-1} - \Sigma_{\bar{\sigma}\bar{\sigma}} - \Sigma_{\bar{\sigma}\sigma}\tilde{G}^0_{\sigma\sigma}\Sigma_{\sigma\bar{\sigma}}]^{-1} \end{bmatrix}. \tag{A2}$$

Equation (9) is the same as Eqs. (5a) and (5b) in Ref. 13 exactly.

APPENDIX B

In order to solve Eq. (4), one has to decouple the two correlation functions $\langle T\{c_{k_\alpha s}d^\dagger_{\bar{\sigma}}d_{\bar{\sigma}}, d^\dagger_\sigma\}\rangle$, $\langle T\{c^\dagger_{k_\alpha s}d_\sigma d_{\bar{\sigma}}, d^\dagger_\sigma\}\rangle$, and $\langle T\{c_{k_\alpha s}d^\dagger_{\bar{\sigma}}d_{\bar{\sigma}}, d^\dagger_\sigma\}\rangle$, etc. The decoupling scheme proposed by Lacroix in the high-temperature limit

$$\langle T\{c^\dagger_{k_\alpha s}(t)c_{k_\beta s'}(t)d_{\bar{\sigma}}(t), d^\dagger_\sigma(t')\}\rangle = \delta_{k_\alpha,k_\beta}\delta_{s,s'}f(\epsilon_{k\alpha s})\langle T\{d_{\bar{\sigma}}(t), d^\dagger_\sigma(t')\}\rangle,$$

$$\langle T\{c^\dagger_{k_\alpha s}(t)c_{k_\beta s'}(t)d_\sigma(t), d^\dagger_\sigma(t')\}\rangle = \delta_{k_\alpha,k_\beta}\delta_{s,s'}f(\epsilon_{k\alpha s})\langle T\{d_\sigma(t), d^\dagger_\sigma(t')\}\rangle,$$

$$\langle T\{c_{k_\alpha s}(t)c_{k_\beta s'}(t)d^\dagger_\sigma(t), d^\dagger_\sigma(t')\}\rangle = \langle T\{c_{k_\alpha s}(t)c_{k_\beta s'}(t)d^\dagger_{\bar{\sigma}}(t), d^\dagger_\sigma(t')\}\rangle = 0 \tag{B1}$$

is used. For example, consider the term $\langle c_{k_\alpha s}d^\dagger_{\bar{\sigma}}d_\sigma, d^\dagger_\sigma\rangle$ of Eq. (4). Using the EOM method, and Lacroix's high-temperature decoupling approximation, one obtains

$$
\begin{aligned}
&(\omega-\epsilon_{k\alpha s}-\epsilon_\sigma+\epsilon_{\bar\sigma})\langle T\{c_{k_{\alpha^s}}d_{\bar\sigma}^\dagger d_\sigma,d_\sigma^\dagger\}\rangle\\
&=V_{k_{\alpha^s},\sigma}\langle T\{d_\sigma d_{\bar\sigma}^\dagger d_\sigma,d_{\bar\sigma}^\dagger\}\rangle+V_{k_{\alpha^s},\bar\sigma}\langle T\{d_{\bar\sigma}d_{\bar\sigma}^\dagger d_\sigma,d_\sigma^\dagger\}\rangle\\
&\quad-\sum_{q\alpha s'}V_{q_{\alpha^{s'}},\bar\sigma}\langle T\{c_{k_{\alpha^s}}c_{q_{\alpha^{s'}}}^\dagger d,d_\sigma^\dagger\}\rangle\\
&=-\langle d_{\bar\sigma}^\dagger d_\sigma\rangle V_{k_{\alpha^s},\sigma}(i)G_{\sigma\sigma}+V_{k_{\alpha^s},\bar\sigma}(i)(G_{\sigma\sigma}-G_{\sigma\sigma}^{(2)})\\
&\quad-\sum_{q\alpha s'}V_{q_{\alpha^{s'}},\bar\sigma}\langle c_{k_{\alpha^s}}c_{q_{\alpha^{s'}}}^\dagger\rangle(i)G_{\sigma\sigma}\delta_{k_{\alpha^s},q_{\alpha^{s'}}};
\end{aligned}
\tag{B2}
$$

thus

$$
\begin{aligned}
&-\sum_{k_\alpha s}V_{k\alpha s,\bar\sigma}^*(-i)\langle c_{k_{\alpha^s}}d_{\bar\sigma}^\dagger d_\sigma,d_\sigma^\dagger\rangle\\
&=\langle d_{\bar\sigma}^\dagger d_\sigma\rangle\sum_{k_\alpha s}\frac{V_{k\alpha s,\bar\sigma}^*V_{k\alpha s,\sigma}}{\omega-\epsilon_{k\alpha s}-\epsilon_\sigma+\epsilon_{\bar\sigma}}G_{\sigma\sigma}\\
&+\sum_{k_\alpha s}\frac{|V_{k\alpha s,\bar\sigma}|^2}{\omega-\epsilon_{k\alpha s}-\epsilon_\sigma+\epsilon_{\bar\sigma}}(G_{\sigma\sigma}^{(2)}-G_{\sigma\sigma})\\
&+\sum_{k_\alpha s}\frac{|V_{k\alpha s,\bar\sigma}|^2}{\omega-\epsilon_{k\alpha s}-\epsilon_\sigma+\epsilon_{\bar\sigma}}[1-f_\alpha(\epsilon_{k\alpha s})]G_{\sigma\sigma}.
\end{aligned}
\tag{B3}
$$

In the same way, the $\langle T\{c_{k_{\alpha^s}}d_{\bar\sigma}^\dagger d_\sigma,d_{\bar\sigma}^\dagger\}\rangle$ term of Eq. (4) is

$$
\begin{aligned}
&\sum_{k_\alpha s}V_{k\alpha s,\sigma}^*(-i)\langle T\{c_{k_{\alpha^s}}d_{\bar\sigma}^\dagger d_\sigma,d_\sigma^\dagger\}\rangle\\
&=\sum_{k_\alpha s}\frac{|V_{k\alpha s,\sigma}|^2}{\omega-\epsilon_{k\alpha s}}G_{\sigma\sigma}^{(2)}-\langle n_{\bar\sigma}\rangle\frac{V_{k\alpha s,\sigma}^*V_{k\alpha s,\bar\sigma}}{\omega-\epsilon_{k\alpha s}}G_{\bar\sigma\sigma}\\
&+\frac{V_{k\alpha s,\sigma}^*V_{k\alpha s,\bar\sigma}}{\omega-\epsilon_{k\alpha s}}f_\alpha(\epsilon_{k\alpha s})G_{\bar\sigma\sigma}
\end{aligned}
\tag{B4}
$$

and the $\langle T\{c_{k_{\alpha^s}}^\dagger d_\sigma d_{\bar\sigma},d_\sigma^\dagger\}\rangle$ term is

$$
\begin{aligned}
&\sum_{k_\alpha s}V_{k\alpha s,\bar\sigma}^*(-i)\langle T\{c_{k_{\alpha^s}}^\dagger d_\sigma d_{\bar\sigma},d_\sigma^\dagger\}\rangle\\
&=\sum_{k_\alpha s}-\frac{|V_{k\alpha s,\sigma}|^2}{\omega+\epsilon_{k\alpha s}-\epsilon_\sigma-\epsilon_{\bar\sigma}-U}G_{\bar\sigma\sigma}^{(2)}\\
&-\frac{|V_{k\alpha s,\sigma}|^2}{\omega+\epsilon_{k\alpha s}-\epsilon_\sigma-\epsilon_{\bar\sigma}-U}G_{\sigma\sigma}^{(2)}\\
&+\sum_{k_\alpha s}\frac{|V_{k\alpha s,\sigma}|^2}{\omega+\epsilon_{k\alpha s}-\epsilon_\sigma-\epsilon_{\bar\sigma}-U}f_\alpha(\epsilon_{k\alpha s})G_{\bar\sigma\sigma}\\
&+\frac{V_{k\alpha s,\bar\sigma}^*V_{k\alpha s,\sigma}}{\omega+\epsilon_{k\alpha s}-\epsilon_\sigma-\epsilon_{\bar\sigma}-U}f_\alpha(\epsilon_{k\alpha s})G_{\sigma\sigma}.
\end{aligned}
\tag{B5}
$$

Under the infinite-U limit, the Eq. (14) is zero. Compare to Eq. (5), The self-energy $Y_{\sigma\bar\sigma}^{(2)}$ transfers $G_{\bar\sigma\sigma}^{(2)}$ to $G_{\sigma\sigma}^{(2)}$, we can recognize that $Y_{\sigma\bar\sigma}^{(2)}=\Sigma_{k_{\alpha^s}}-|V_{k\alpha s,\sigma}|^2/(\omega+\epsilon_{k\alpha s}-\epsilon_\sigma-\epsilon_{\bar\sigma}-U)$ and can be ignored under the infinite-U limit. Hence the Green's function $G_{\sigma\sigma}^{(2)}$ is found as

$$
\begin{aligned}
&(\omega-\epsilon_\sigma-U)G_{\sigma\sigma}^{(2)}(\omega)\\
&=n_{\bar\sigma}+\sum_{k_\alpha s}\frac{|V_{k\alpha s,\sigma}|^2}{\omega-\epsilon_{k\alpha s}}G_{\sigma\sigma}^{(2)}-\langle n_{\bar\sigma}\rangle\frac{V_{k\alpha s,\sigma}^*V_{k\alpha s,\bar\sigma}}{\omega-\epsilon_{k\alpha s}}G_{\bar\sigma\sigma}\\
&+\frac{V_{k\alpha s,\sigma}^*V_{k\alpha s,\bar\sigma}}{\omega-\epsilon_{k\alpha s}}f_\alpha(\epsilon_{k\alpha s})G_{\bar\sigma\sigma}+\langle d_{\bar\sigma}^\dagger d_\sigma\rangle\\
&\sum_{k_\alpha s}\frac{V_{k\alpha s,\bar\sigma}^*V_{k\alpha s,\sigma}}{\omega-\epsilon_{k\alpha s}-\epsilon_\sigma+\epsilon_{\bar\sigma}}G_{\sigma\sigma}+\frac{|V_{k\alpha s,\bar\sigma}|^2}{\omega-\epsilon_{k\alpha s}-\epsilon_\sigma+\epsilon_{\bar\sigma}}(G_{\sigma\sigma}^{(2)}\\
&-G_{\sigma\sigma})+\frac{|V_{k\alpha s,\bar\sigma}|^2}{\omega-\epsilon_{k\alpha s}-\epsilon_\sigma+\epsilon_{\bar\sigma}}[1-f_\alpha(\epsilon_{k\alpha s})]G_{\sigma\sigma}\equiv Y_{\sigma\sigma}^{(2)}G_{\sigma\sigma}^{(2)}\\
&+X_{\sigma\sigma}^{(2)}G_{\sigma\sigma}+X_{\sigma\bar\sigma}^{(2)}G_{\bar\sigma\sigma}
\end{aligned}
\tag{B6}
$$

where

$$
Y_{\sigma\sigma}^{(2)}\equiv\sum_{k_\alpha s}\frac{|V_{k\alpha s,\sigma}|^2}{\omega-\epsilon_{k\alpha s}}+\frac{|V_{k\alpha s,\bar\sigma}|^2}{\omega-\epsilon_{k\alpha s}-\epsilon_\sigma+\epsilon_{\bar\sigma}},
$$

$$
\begin{aligned}
X_{\sigma\sigma}^{(2)}&\equiv\sum_{k_\alpha s}\langle d_{\bar\sigma}^\dagger d_\sigma\rangle\frac{V_{k\alpha s,\sigma}^*V_{k\alpha s,\bar\sigma}}{\omega-\epsilon_{k\alpha s}-\epsilon_\sigma+\epsilon_{\bar\sigma}}\\
&\quad-\frac{|V_{k\alpha s,\bar\sigma}|^2}{\omega-\epsilon_{k\alpha s}-\epsilon_\sigma+\epsilon_{\bar\sigma}}f_\alpha(\epsilon_{k\alpha s}),
\end{aligned}
$$

$$
X_{\sigma\bar\sigma}^{(2)}=\sum_{k_\alpha s}-\langle n_{\bar\sigma}\rangle\frac{V_{k\alpha s,\sigma}^*V_{k\alpha s,\bar\sigma}}{\omega-\epsilon_{k\alpha s}}+\frac{V_{k\alpha s,\sigma}^*V_{k\alpha s,\bar\sigma}}{\omega-\epsilon_{k\alpha s}}f_\alpha(\epsilon_{k\alpha s}).
\tag{B7}
$$

APPENDIX C

In this appendix, we will show the detailed derivation of the expressions for $\langle n_\sigma\rangle$ and $\langle n_{\bar\sigma\sigma}\rangle$. We follow the derivation proposed by Sun and Guo. Since the system considered in this paper is in steady state, the first derivation of the expectation values of $\langle d_\sigma^\dagger d_\sigma\rangle$ and $\langle d_{\bar\sigma}^\dagger d_\sigma\rangle$ over time is zero, i.e., $\langle i(\partial/\partial t)[d_\sigma^\dagger d_\sigma]\rangle=0$. Using the equation of motion method, one can find the time evolution of particle number $\langle d_\sigma^\dagger d_\sigma\rangle$ as

Hence,

$$
\left\langle i\frac{\partial}{\partial t}[d_\sigma^\dagger d_\sigma]\right\rangle=\sum_{k\alpha s}-V_{k\alpha s,\sigma}\langle c_{k\alpha s}^\dagger d_\sigma\rangle+V_{k\alpha s,\sigma}^*\langle d_\sigma^\dagger c_{k\alpha s}\rangle=0
\tag{C1}
$$

where $\langle c_{k\alpha s}^\dagger d_\sigma\rangle=-i\int(d\epsilon/2\pi)G_{\sigma,k\alpha s}^<(\varepsilon)$ and $\langle d_\sigma^\dagger c_{k\alpha s}\rangle=-i\int(d\epsilon/2\pi)G_{k\alpha s,\sigma}^<(\varepsilon)$. The lesser Green's functions $G_{\sigma,k\alpha s}^<(\varepsilon)$ and $G_{k\alpha s,\sigma}^<(\varepsilon)$ can be easily calculated by the Dyson expansion and Langreth theorem. In order to calculate the lesser Green's function, the contour-ordered Green's function must be found first. The contour Green's function $G_{k\alpha s,\sigma}(t,t')$ is

$$G_{k\alpha s,\sigma}(t,t') = -iT\langle c_{k\alpha s}(t)d^{\dagger}_{\sigma}(t')\rangle$$
$$= (-i)^2 T\int d\tau[V_{k\alpha s,\sigma}\langle c_{k\alpha s}(t)c^{\dagger}_{k\alpha s}(\tau)\rangle\langle d_{\sigma}d^{\dagger}_{\sigma}(t')\rangle$$
$$+ V_{k\alpha s,\bar{\sigma}}\langle c_{k\alpha s}(t)c^{\dagger}_{k\alpha s}(\tau)\rangle\langle d_{\bar{\sigma}}d^{\dagger}_{\sigma}(t')\rangle]$$
$$= T\int d\tau[V_{k\alpha s,\sigma}g_{k\alpha s}(t,\tau)G_{\sigma\sigma}(\tau,t')$$
$$+ V_{k\alpha s,\bar{\sigma}}g_{k\alpha s}(t,\tau)G_{\bar{\sigma}\sigma}(\tau,t')]. \quad \text{(C2)}$$

Then, using the Fourier transformation and Langreth theorem, the lesser Green's function $G^{<}_{k\alpha s,\sigma}$ is obtained:

$$G^{<}_{k\alpha s,\sigma} = V_{k\alpha s,\sigma}(g^{r}_{k\alpha s}G^{<}_{\sigma\sigma} + g^{<}_{k\alpha s}G^{a}_{\sigma\sigma}) + V_{k\alpha s,\bar{\sigma}}(g^{r}_{k\alpha s}G^{<}_{\bar{\sigma}\sigma}$$
$$+ g^{<}_{k\alpha s}G^{a}_{\bar{\sigma}\sigma}). \quad \text{(C3)}$$

In the same way, the lesser Green's function $G^{<}_{\sigma,k\alpha s}$ is

$$G^{<}_{\sigma,k\alpha s} = V^{*}_{k\alpha s,\sigma}(G^{r}_{\sigma\sigma}g^{<}_{k\alpha s} + G^{<}_{\sigma\sigma}g^{a}_{k\alpha s}) + V^{*}_{k\alpha s,\bar{\sigma}}(G^{r}_{\sigma\bar{\sigma}}g^{<}_{k\alpha s}$$
$$+ G^{<}_{\sigma\bar{\sigma}}g^{a}_{k\alpha s}). \quad \text{(C4)}$$

Substituting Eqs. (C3) and (C4) into Eq. (C1), one can obtain

$$\sum_{k_{\alpha}s}\int\frac{d\epsilon}{2\pi}V^{*}_{k_{\alpha}s,\sigma}V_{k_{\alpha}s,\sigma}[G^{r}_{\sigma\sigma}g^{<}_{k_{\alpha}s}(\epsilon) + G^{<}_{\sigma\sigma}(\epsilon)g^{a}_{k_{\alpha}s}(\epsilon)]$$
$$+ V^{*}_{k_{\alpha}s,\bar{\sigma}}V_{k_{\alpha}s,\sigma}[G^{r}_{\sigma\bar{\sigma}}(\epsilon)g^{<}_{k_{\alpha}s} + G^{<}_{\sigma\bar{\sigma}}(\epsilon)g^{a}_{k_{\alpha}s}]$$
$$= \sum_{k_{\alpha}s}\int\frac{d\epsilon}{2\pi}V^{*}_{k_{\alpha}s,\sigma}V_{k_{\alpha}s,\sigma}(g^{r}_{k_{\alpha}s}G^{<}_{\sigma\sigma} + g^{<}_{k_{\alpha}s}G^{a}_{\sigma\sigma})$$
$$+ V^{*}_{k_{\alpha}s,\bar{\sigma}}V_{k_{\alpha}s,\sigma}(g^{r}_{k_{\alpha}s}G^{<}_{\bar{\sigma}\sigma} + g^{<}_{k_{\alpha}s}G^{a}_{\bar{\sigma}\sigma}). \quad \text{(C5)}$$

Using the relations $\Sigma_{k_{\alpha}s}V^{*}_{k_{\alpha}s,\sigma}V_{k_{\alpha}s,\sigma}g^{r,a}_{k_{\alpha}s} = \Sigma_{\alpha}\mp i(\Gamma^{\alpha}_{n}/2)$, $\Sigma_{k_{\alpha}s}V^{*}_{k_{\alpha}s,\bar{\sigma}}V_{k_{\alpha}s,\sigma}g^{r,a}_{k_{\alpha}s} = \Sigma_{\alpha}\mp i(\Gamma^{\alpha}_{s}/2)$, $\Sigma_{k_{\alpha}s}V^{*}_{k_{\alpha}s,\sigma}V_{k_{\alpha}s,\sigma}g^{<}_{k_{\alpha}s}(\epsilon) = i\Sigma_{\alpha}\Gamma^{\alpha}_{n}f_{\alpha}(\epsilon)$, and $\Sigma_{k_{\alpha}s}V^{*}_{k_{\alpha}s,\bar{\sigma}}V_{k_{\alpha}s,\sigma}g^{<}_{k\alpha s}(\epsilon) = i\Sigma_{\alpha}\Gamma^{\alpha}_{s}f_{\alpha}(\epsilon)$, and after some simple algebra, one finds

$$(\Gamma^{2}_{n} - \Gamma^{2}_{s})\int\frac{d\epsilon}{2\pi}G^{<}_{\sigma\sigma}(\epsilon)$$
$$= \Gamma_{n}\left(\sum_{\alpha} -i\Gamma^{\alpha}_{n}\int\frac{d\epsilon}{2\pi}f_{\alpha}(\epsilon)[2\ \mathrm{Im}\ G^{r}_{\sigma\sigma}(\epsilon)]\right.$$
$$\left. - i\Gamma^{\alpha}_{s}\int\frac{d\epsilon}{2\pi}f_{\alpha}(\epsilon)[2\ \mathrm{Im}\ G^{r}_{\bar{\sigma}\sigma}(\epsilon)]\right)$$
$$- \Gamma_{s}\left(\sum_{\alpha} -i\Gamma^{\alpha}_{s}\int\frac{d\epsilon}{2\pi}f_{\alpha}(\epsilon)[2\ \mathrm{Im}\ G^{r}_{\sigma\sigma}(\epsilon)]\right.$$
$$\left. - i\Gamma^{\alpha}_{n}\int\frac{d\epsilon}{2\pi}f_{\alpha}(\epsilon)[2\ \mathrm{Im}\ G^{r}_{\bar{\sigma}\sigma}(\epsilon)]\right) \quad \text{(C6)}$$

where $\Gamma_{n} = \Sigma_{\alpha}\Gamma^{\alpha}_{n}$ and $\Gamma_{s} = \Sigma_{\alpha}\Gamma^{\alpha}_{s}$. In Eq. (C6), we have used the relation $G^{r,a,<}_{\bar{\sigma}\sigma}(\epsilon) = G^{r,a,<}_{\sigma\bar{\sigma}}(\epsilon)$ since the spin states are degenerate in the QD. In the same way for treating $\langle i(\partial/\partial t)\times[d^{\dagger}_{\sigma}d_{\sigma}]\rangle = 0$, with the condition $\langle i(\partial/\partial t)[d^{\dagger}_{\bar{\sigma}}d_{\sigma}]\rangle = 0$, one obtains the relation

$$(\Gamma^{2}_{n} - \Gamma^{2}_{s})\int\frac{d\epsilon}{2\pi}G^{<}_{\bar{\sigma}\sigma}(\epsilon)$$
$$= \Gamma_{n}\left(\sum_{\alpha} -i\Gamma^{\alpha}_{s}\int\frac{d\epsilon}{2\pi}f_{\alpha}(\epsilon)[2\ \mathrm{Im}\ G^{r}_{\sigma\sigma}(\epsilon)]\right.$$
$$\left. - i\Gamma^{\alpha}_{n}\int\frac{d\epsilon}{2\pi}f_{\alpha}(\epsilon)[2\ \mathrm{Im}\ G^{r}_{\bar{\sigma}\sigma}(\epsilon)]\right)$$
$$- \Gamma_{s}\left(\sum_{\alpha} -i\Gamma^{\alpha}_{n}\int\frac{d\epsilon}{2\pi}f_{\alpha}(\epsilon)\big[2\ \mathrm{Im}\ G^{r}_{\sigma\sigma}(\epsilon)\big]\right.$$
$$\left. - i\Gamma^{\alpha}_{s}\int\frac{d\epsilon}{2\pi}f_{\alpha}(\epsilon)[2\ \mathrm{Im}G^{r}_{\bar{\sigma}\sigma}(\epsilon)]\right). \quad \text{(C7)}$$

Since the retarded (advanced) Green's functions have been solved, the equations for $\int(d\epsilon/2\pi)G^{<}_{\sigma\sigma}(\epsilon)$ and $\int(d\epsilon/2\pi)G^{<}_{\bar{\sigma}\sigma}(\epsilon)$ can be solved also. The results can be checked by taking the equilibrium limit, i.e., $f_{R}(\epsilon) = f_{L}(\epsilon) = f(\epsilon)$,

$$\langle n_{\sigma}\rangle = -i\int\frac{d\epsilon}{2\pi}G^{<}_{\sigma\sigma}(\epsilon) = \int\frac{d\epsilon}{2\pi}f_{\alpha}(\epsilon)[-2\ \mathrm{Im}\ G^{r}_{\sigma\sigma}(\epsilon)] \quad \text{(C8)}$$

and

$$\langle d^{\dagger}_{\bar{\sigma}}d_{\sigma}\rangle = -i\int\frac{d\epsilon}{2\pi}G^{<}_{\bar{\sigma}\sigma}(\epsilon) = \int\frac{d\epsilon}{2\pi}f_{\alpha}(\epsilon)[-2\ \mathrm{Im}\ G^{r}_{\bar{\sigma}\sigma}(\epsilon)]. \quad \text{(C9)}$$

Equations (C8) and (C9) show that Eqs. (C6) and (C7) obey the fluctuation-dissipation theorem at the equilibrium limit:

$$\Gamma_{n}\int\frac{d\epsilon}{2\pi}G^{<}_{\sigma\sigma}(\epsilon) + \Gamma_{s}\int\frac{d\epsilon}{2\pi}G^{<}_{\sigma\bar{\sigma}}(\epsilon)$$
$$= \sum_{\alpha} -\Gamma^{\alpha}_{n}\int\frac{d\epsilon}{2\pi}f_{\alpha}(\epsilon)[G^{r}_{\sigma\sigma}(\epsilon) - G^{a}_{\sigma\sigma}(\epsilon)]$$
$$- \Gamma^{\alpha}_{s}\int\frac{d\epsilon}{2\pi}f_{\alpha}(\epsilon)[G^{r}_{\bar{\sigma}\sigma}(\epsilon) - G^{a}_{\bar{\sigma}\sigma}(\epsilon)], \quad \text{(C10)}$$

$$\Gamma_{s}\int\frac{d\epsilon}{2\pi}G^{<}_{\sigma\sigma}(\epsilon) + \Gamma_{n}\int\frac{d\epsilon}{2\pi}G^{<}_{\sigma\bar{\sigma}}(\epsilon)$$
$$= \sum_{\alpha} -\Gamma^{\alpha}_{s}\int\frac{d\epsilon}{2\pi}f_{\alpha}(\epsilon)[G^{r}_{\sigma\sigma}(\epsilon) - G^{a}_{\sigma\sigma}(\epsilon)]$$
$$- \Gamma^{\alpha}_{n}\int\frac{d\epsilon}{2\pi}f_{\alpha}(\epsilon)[G^{r}_{\sigma\sigma}(\epsilon) - G^{a}_{\sigma\bar{\sigma}}(\epsilon)]. \quad \text{(C11)}$$

[1] M. Dax, Semicond. Int. **20**, 84 (1997).
[2] H. X. Tang, F. G. Monzon, Ron Lifshitz, M. C. Cross, and M. L. Roukes, Phys. Rev. B **61**, 4437 (2000); X. F. Wang, P. Vasilopoulos and F. M. Peeters, *ibid.* **65**, 165217 (2002).
[3] B. E. Kane, Nature (London) **393**, 133 (1998).
[4] S. Bandyopadhyay, Phys. Rev. B **61**, 13813 (2000).
[5] F. Guinea, Phys. Rev. B **58**, 9212 (1998).
[6] A. V. Akimov, A. V. Scherbakov, D. R. Yakovlev, W. Ossau, L. W. Molenkamp, T. Wojtowicz, J. Kossut, S. Tatarenko, and J. Cibert, Physica B **316-317**, 41 (2002).
[7] F. T. Vasko and O. Keller, Phys. Rev. B **58**, 15666 (1998).
[8] P. Zhang, Q. K. Xue, Y. P. Wang, and X. C. Xie, Phys. Rev. Lett. **89**, 286803 (2002).
[9] N. Sergueev, Qing-feng Sun, Hong Guo, B. G. Wang, and Jian Wang, Phys. Rev. B **65**, 165303 (2002).
[10] J. Martinek, Y. Utsumi, H. Imamura, J. Barnas, S. Maekawa, J. Konig, and G. Schon, Phys. Rev. Lett. **91**, 127203 (2003).
[11] Bing Dong, H. L. Cui, S. Y. Liu, and X. L. Lei, J. Phys.: Condens. Matter **15**, 8435 (2003).
[12] J. Martinek, M. Sindel, L. Borda, J. Barnas, J. Konig, G. Schon, and J. von Delft, Phys. Rev. Lett. **91**, 247202 (2003).
[13] Jian-Xin Zhu and A. V. Balatsky, Phys. Rev. Lett. **89**, 286802 (2002).
[14] L. I. Glazman and M. E. Raikh, Pis'ma Zh. Eksp. Teor. Fiz. **47**, 378 (1988) [JETP Lett. **47**, 452 (1988)]; Tai Kai Ng and Patrick A. Lee, Phys. Rev. Lett. **61**, 1768 (1988).
[15] P. W. Anderson, Phys. Rev. **124**, 41 (1961).
[16] L. Kouwenhoven and L. Glazman, Phys. World **14** (1), 33 (2001).
[17] J. R. Schrieffer and P. A. Wolff, Phys. Rev. **149**, 491 (1966).
[18] Ned S. Wingreen, and Yigal Meir, Phys. Rev. B **49**, 11040 (1994).
[19] C. Lacroix, J. Phys. F: Met. Phys. **11**, 2389 (1981).
[20] Yigal Meir, Ned S. Wingreen, and Patrick A. Lee, Phys. Rev. Lett. **70**, 2601 (1993).
[21] Kicheon Kang and B. I. Min, Phys. Rev. B **52**, 10689 (1995).
[22] H.-G. Luo, Z.-J. Ying, and S.-J. Wang, Phys. Rev. B **59**, 9710 (1999).
[23] T. A. Costi, A. C. Hewson, and V. Zlatic, J. Phys.: Condens. Matter **6**, 2519 (1994).
[24] Qing-feng Sun and Hong Guo, Phys. Rev. B **66**, 155308 (2002).
[25] Antti-Pekka Jauho, Ned S. Wingreen, and Yigal Meir, Phys. Rev. B **50**, 5528 (1994).
[26] F. D. M. Haldane, Ph.D. thesis, University of Cambridge, 1987; Phys. Rev. Lett. **40**, 416 (1978).
[27] The temperature of interest in Ref. 20 is an order of 2 lower than the Kondo temperature; however, the temperature considered in our work is about one-tenth of the Kondo temperature, Therefore, our decoupling approach sounds reasonable.